







## PRIMARY RESEARCH ARTICLE

# Maximum carbon uptake rate dominates the interannual variability of global net ecosystem exchange

Zheng Fu<sup>1,2</sup>  | Paul C. Stoy<sup>3</sup>  | Benjamin Poulter<sup>4</sup>  | Tobias Gerken<sup>5</sup>  |  
Zhen Zhang<sup>6</sup>  | Guta Wakbulcho<sup>3</sup> | Shuli Niu<sup>1,2</sup> 

<sup>1</sup>Key Laboratory of Ecosystem Network Observation and Modeling, Institute of Geographic Sciences and Natural Resources Research, Chinese Academy of Sciences, Beijing, China

<sup>2</sup>University of Chinese Academy of Sciences, Beijing, China

<sup>3</sup>Department of Land Resources and Environmental Sciences, Montana State University, Bozeman, Montana

<sup>4</sup>Biospheric Sciences Laboratory, NASA Goddard Space Flight Center, Greenbelt, Maryland

<sup>5</sup>Department of Meteorology and Atmospheric Science, The Pennsylvania State University, University Park, Pennsylvania

<sup>6</sup>Department of Geographical Sciences, University of Maryland, College Park, Maryland

## Correspondence

Shuli Niu, Synthesis Research Center of Chinese Ecosystem Research Network, Key Laboratory of Ecosystem Network Observation and Modeling, Institute of Geographic Sciences and Natural Resources Research, Chinese Academy of Sciences, Beijing 100101, China.  
Email: sniu@igsrr.ac.cn

## Funding information

National Key R & D Program of China, Grant/Award Number: 2018YFA0606102; National Natural Science Foundation of China, Grant/Award Number: 31625006; Chinese Academy of Sciences, Grant/Award Number: 131A11KYSB20180010; Gordon and Betty Moore Foundation, Grant/Award Number: GBMF5439; NASA Terrestrial Ecology Program; National Science Foundation, Grant/Award Number: DEB 1552976, OIA 1632810 and EF 1702029; USDA-NIFA, Grant/Award Number: 228396

## Abstract

Terrestrial ecosystems contribute most of the interannual variability (IAV) in atmospheric carbon dioxide (CO<sub>2</sub>) concentrations, but processes driving the IAV of net ecosystem CO<sub>2</sub> exchange (NEE) remain elusive. For a predictive understanding of the global C cycle, it is imperative to identify indicators associated with ecological processes that determine the IAV of NEE. Here, we decompose the annual NEE of global terrestrial ecosystems into their phenological and physiological components, namely maximum carbon uptake (MCU) and release (MCR), the carbon uptake period (CUP), and two parameters,  $\alpha$  and  $\beta$ , that describe the ratio between actual versus hypothetical maximum C sink and source, respectively. Using long-term observed NEE from 66 eddy covariance sites and global products derived from FLUXNET observations, we found that the IAV of NEE is determined predominately by MCU at the global scale, which explains 48% of the IAV of NEE on average while  $\alpha$ , CUP,  $\beta$ , and MCR explain 14%, 25%, 2%, and 8%, respectively. These patterns differ in water-limited ecosystems versus temperature- and radiation-limited ecosystems; 31% of the IAV of NEE is determined by the IAV of CUP in water-limited ecosystems, and 60% of the IAV of NEE is determined by the IAV of MCU in temperature- and radiation-limited ecosystems. The Lund-Potsdam-Jena (LPJ) model and the Multi-scale Synthesis and Terrestrial Model Inter-comparison Project (MsTMIP) models underestimate the contribution of MCU to the IAV of NEE by about 18% on average, and overestimate the contribution of CUP by about 25%. This study provides a new perspective on the proximate causes of the IAV of NEE, which suggest that capturing the variability of MCU is critical for modeling the IAV of NEE across most of the global land surface.

## KEYWORDS

carbon uptake period, interannual variability, maximum carbon uptake rate, net ecosystem exchange, phenology, physiology

## 1 | INTRODUCTION

The large year-to-year variation in the growth rate of atmospheric carbon dioxide ( $\text{CO}_2$ ) is due primarily to the interannual variability (IAV) of the terrestrial carbon cycle rather than the oceanic C cycle (Le Quéré et al., 2018). The causes for the IAV of terrestrial C cycle differ across different global regions and scales of observation (Jung et al., 2017) and models have difficulty replicating it (Keenan et al., 2012; Niu et al., 2017), indicating a fundamental gap in our understanding. Temperature (Wang et al., 2014), precipitation (Jung et al., 2017; Poulter et al., 2014), and solar radiation (Ichii, Hashimoto, Nemani, & White, 2005; Nemani et al., 2003) have been reported as the most important climate factors in controlling the IAV of the terrestrial C cycle in different ecosystems, but the biological mechanisms underlying the IAV of net ecosystem  $\text{CO}_2$  exchange (NEE) at the global scale are far from clear. It is imperative to identify the drivers associated with underlying ecological processes that determine the IAV of NEE for an improved predictive understanding of the global C cycle.

The variation of NEE results from the small imbalance between two larger fluxes: the photosynthetic uptake of  $\text{CO}_2$  (gross primary production, GPP) and the respiratory release of  $\text{CO}_2$  from autotrophic and heterotrophic processes (ecosystem respiration, ER). Annual GPP is easily decomposed into different processes; for example, 90% of its annual variability can be explained by the product of the maximum daily GPP ( $\text{GPP}_{\text{max}}$ ) and growing season length in temperate and boreal ecosystems (Xia et al., 2015; Zhou et al., 2016). These findings rely on the notion that the seasonality of GPP follows a fundamental unifying pattern across different vegetation types and highlight the important role of  $\text{GPP}_{\text{max}}$  and growing season length in controlling plant  $\text{CO}_2$  uptake, although it is unclear if these indicators related to plant C uptake emerge to be the most important controls over the IAV of NEE. As far as we know, a decomposition of the indicators that contribute to annual global NEE has not been studied to date, especially in the southern hemisphere where biomes such as tropical forests, savanna, and Mediterranean ecosystems are dominant.

Extending the net carbon uptake period (CUP) likely, but not necessarily, leads to larger net C uptake (Churkina, Schimel, Braswell, & Xiao, 2005; Dragoni et al., 2011; Richardson et al., 2013). An increase in the maximum net C uptake/release rate tends to stimulate/reduce annual net C uptake as well (Fu, Dong, Zhou, Stoy, & Niu, 2017; Zscheischler et al., 2016). Changes in the maximum net carbon uptake/release and the length of net CUP are thus likely to co-contribute to the variability in annual NEE (Figure 1). Unlike  $\text{GPP}_{\text{max}}$  and growing season length (Xia et al., 2015; Zhou et al., 2016), the maximum net carbon uptake/release and net CUP contain the signals of both photosynthesis and respiration, which more directly reflect the net carbon uptake at the ecosystem level. As the maximum net carbon uptake/release represents important characteristics of photosynthesis and respiration, it can be used as an indicator of physiology while the net CUP can be used as an indicator of net C uptake phenology. These indicators represent different mechanisms about how net carbon uptake phenology and physiology regulate the IAV of NEE.

Other indicators that are necessary to describe net C uptake and release include the ratio between actual versus hypothetical maximum C sink during the growing season and the ratio between actual versus hypothetical maximum C source (Figure 1). These indicators reflect how much C uptake and loss are constrained by environmental drivers in a given year, respectively, which also contribute to the IAV of NEE. However, it is unclear how much the IAV in NEE is attributed to the changes in the maximum net carbon uptake/release, net CUP and the ratios of actual to hypothetical maximum C sink and source, and what is the relative importance of these indicators across different ecosystems and climate zones globally. Exploring the relative contributions of these indicators will elucidate the contributions of phenological and physiological changes to annual NEE variability and improve our understanding of the IAV of NEE at global scale. Furthermore, the distribution of their relative contributions may be connected to local climate conditions, such as water, temperature, and radiation, because local climate conditions drive the seasonal dynamics of NEE and impact the indicators related to phenology and physiology (Chapin III, Matson, & Vitousek, 2011). However, the effects of climatic drivers in controlling the distribution of their relative contributions remain unclear. We hypothesize that the relative contributions of phenological and physiological indicators to the IAV of NEE may be different among water-limited, temperature-limited, and radiation-limited ecosystems. Changing CUP by a few days may not considerably affect annual net C uptake in temperature-limited ecosystems with a single period of C uptake per growing season (e.g., boreal and temperate ecosystems) because net C uptake strength around the C sink/source transition days tends to be small. However, in water-limited ecosystems, changes in CUP—often due to precipitation events—may appreciably change annual C uptake (Ahlström et al., 2015; Poulter et al., 2014).

To better predict the IAV of terrestrial NEE in a changing climate, it is critical to accurately simulate the roles of phenological and physiological indicators in controlling the IAV of NEE. In recent decades, land surface models have incorporated more and more processes in an attempt to simulate C cycle processes as realistically as possible (Luo et al., 2017; Oleson et al., 2010), however, it is far from clear whether land surface models can capture the contributions of these indicators to the IAV of NEE or not. Comparing results calculated from model outputs with observations allow us to investigate the performance of current land surface models and highlight future directions for improving model predictive skills.

In this study, we used global databases of eddy covariance observations at the site scale and global terrestrial NEE data products that fuse eddy covariance and remote-sensing observations using three different machine learning techniques, FLUXCOM (Jung et al., 2017), to study how phenological and physiological indicators determine the IAV of NEE in terrestrial ecosystems. We also compared the results calculated from FLUXCOM observations with that of the LPJ model and ensemble of Multi-scale Synthesis and Terrestrial Model Inter-comparison Project (MsTMIP) models to see whether the land surface models can capture the observed role of phenological and physiological indicators in controlling the IAV of NEE. The specific

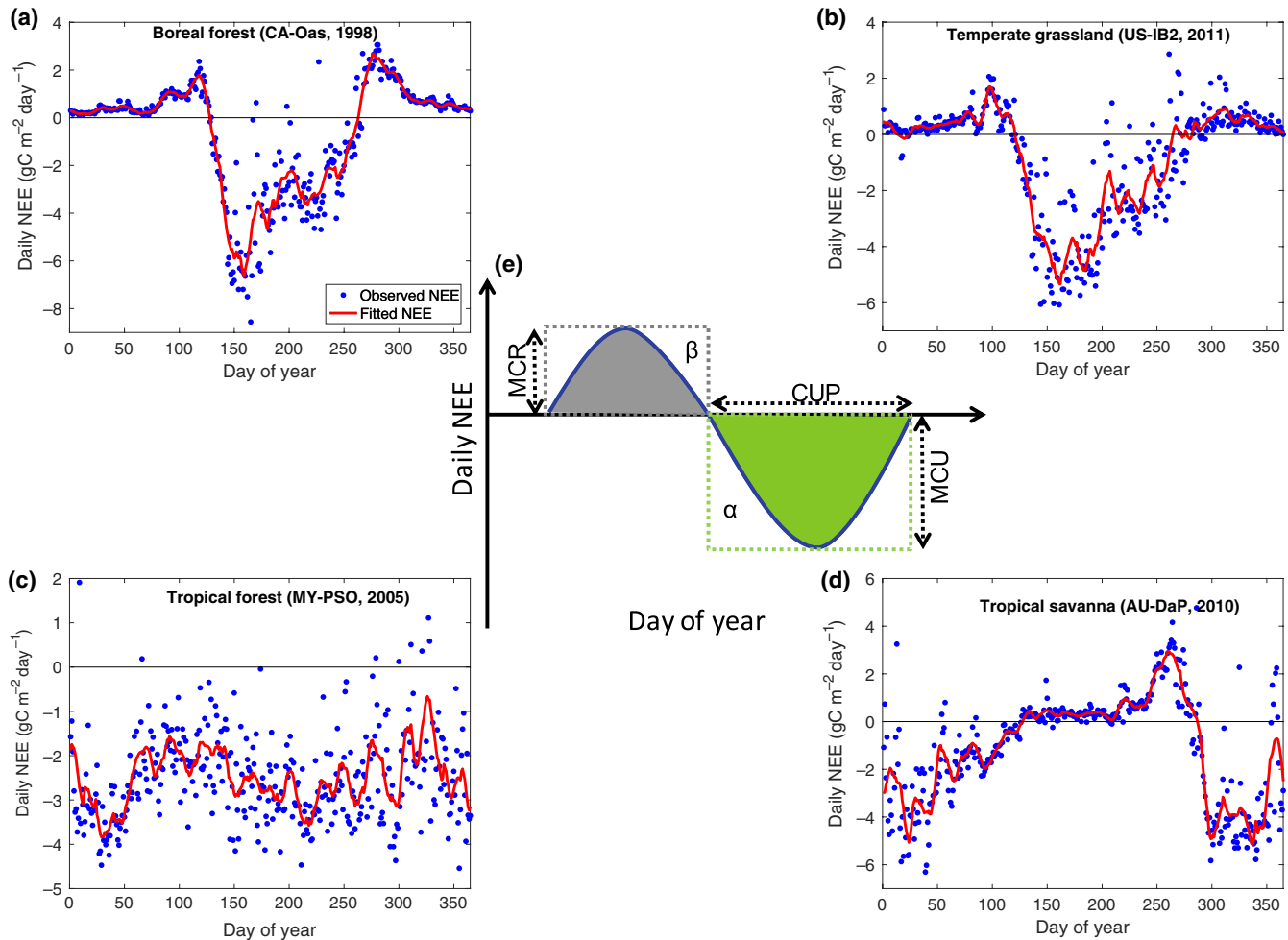


**FIGURE 1** Conceptual figure of  $\alpha$ , maximum CO<sub>2</sub> uptake (MCU), CO<sub>2</sub> uptake period (CUP),  $\beta$ , and maximum CO<sub>2</sub> release (MCR) in determining the changes in annual net ecosystem CO<sub>2</sub> exchange (NEE) (e) with examples of the annual course of observed and filtered NEE (a–d) from different eddy covariance sites (Table S1).  $\alpha$  is the ratio of actual carbon sink and hypothetical maximum carbon sink in a year defined as the simple product of CUP  $\times$  MCU, and  $\beta$  is the ratio of actual carbon source and hypothetical maximum carbon source, that is, the length of the calendar year minus CUP, multiplied by MCR. We applied the Savitzky–Golay filter to minimize the role of random variability in flux observations (Savitzky & Golay, 1964) and calculated  $\alpha$ , MCU, CUP,  $\beta$ , and MCR for each site or grid (see Materials and Methods) [Colour figure can be viewed at [wileyonlinelibrary.com](https://onlinelibrary.wiley.com)]

objectives are to (a) characterize the global patterns of these phenological and physiological indicators; (b) partition their relative contributions to the IAV of NEE across different global ecosystems; and (c) evaluate whether land surface models can capture their relative contributions. To do so, we decompose annual NEE into phenological and physiological indicators that determine it, namely maximum rates of net carbon uptake (MCU) and release (MCR), the net uptake period (CUP), and two parameters,  $\alpha$  and  $\beta$ , that describe the ratio between actual versus hypothetical maximum C sink and source, respectively (Figure 1).

## 2 | MATERIALS AND METHODS

### 2.1 | Datasets

Net ecosystem exchange (NEE) observations from eddy covariance data were retrieved from the FLUXNET2015 dataset.

FLUXNET2015 contains daily averages of CO<sub>2</sub>, water vapor, and energy fluxes that are harmonized, standardized, and gap-filled (Chu, Baldocchi, John, Wolf, & Reichstein, 2017; Papale et al., 2006; Reichstein et al., 2005). Study sites were chosen according to the following two criteria. (a) Only site-years with which more than 80% of the NEE data were measured or gap-filled with high confidence (i.e., data marked as “the original” or “most reliable” according to the quality flag, were selected; in other words, only the site-years at least 292 days of high-quality flux measurements or estimates were used). (b) Sites with a minimum of 5 years of observations were selected. A subset of 66 sites satisfied the two criteria, among which there were 19 evergreen needleleaf forests, three evergreen broadleaf forests, 11 deciduous broadleaf forests, five mixed forests, 10 grasslands, nine croplands, three sites with closed and open shrublands, two wetlands, and four sites with savannas or woody savannas (Table S1).

The three FLUXCOM datasets are built with three machine learning techniques (Random Forests, Artificial Neural Networks, Multivariate Adaptive Regression Splines) to upscale flux observations from FLUXNET in space and time and integrate these with climate and remote-sensing data for the period 1980–2013 (Jung et al., 2011, 2017; Tramontana et al., 2016). Global maps of NEE from three FLUXCOM datasets at 0.5° spatial resolution and daily temporal resolution were used individually, and then the median was taken based on these three results for analysis.

NEE datasets from Lund-Potsdam-Jena (LPJ) dynamic global vegetation model and the MstMIP outputs were also used to evaluate whether land surface models capture the relative contributions of  $\alpha$ , MCU, CUP,  $\beta$ , and MCR to the IAV of NEE. We simulated the daily NEE from 1980 to 2013 with a spatial resolution of 0.5° using LPJ (Sitch et al., 2003) to match with the studied period of the FLUXCOM datasets (1980–2013). The MstMIP provides the three hourly NEE over 7 years (2004–2010) at spatial resolutions of 0.5° × 0.5° ([https://daac.ornl.gov/CMS/guides/CMS\\_CO2\\_Fluxes\\_TBMO.html](https://daac.ornl.gov/CMS/guides/CMS_CO2_Fluxes_TBMO.html)). The three hourly NEE were derived from monthly NEE outputs from the weighted ensemble mean NEE in MstMIP (the 15 MstMIP models included: BIOME\_BGC, CLM, CLM4VIC, CLASS\_CTEM, DLEM, GTEC, ISAM, an earlier version of LPJ, ORCHIDEE, SIB3, SIBCASA, TEM6, TRIPLEX-GHG, VEGAS, and VISIT; Huntzinger et al., 2013; Wei et al., 2014). The three hourly NEE data were aggregated to daily totals.

To analyze the role of climatic drivers in controlling the distribution of relative contributions in the  $\alpha$ , MCU, CUP,  $\beta$ , and MCR, global maps of temperature, water, and radiation constraints to plant growth derived from long-term climate statistics were used (Nemani et al., 2003). The MODIS MCD12C1 land-cover product was used to classify the land pixels and to calculate statistics by IGBP vegetation classes (Friedl & Brodley, 1997). MCD12C1 provides the dominant land-cover types at a spatial resolution of 0.05° using a supervised classification algorithm that is calibrated using a database of land-cover training sites. We remapped using a majority filter to a spatial resolution of 0.5° (Figure S1; Marcolla, Rödenbeck, & Cescatti, 2017).

## 2.2 | Definitions and calculations for $\alpha$ , MCU, CUP, $\beta$ and MCR

We used the daily NEE for each site or grid to calculate  $\alpha$ , MCU, CUP,  $\beta$ , and MCR (Figure 1) and applied the Savitzky–Golay filter to minimize the role of random variability in flux observations (Savitzky & Golay, 1964). The sign convention of NEE is from the perspective of the atmosphere such that NEE is negative for ecosystem C uptake and positive for C release to the atmosphere (Figure 1; Chapin et al., 2006). We defined the CUP as the number of days with net C uptake ( $NEE < 0 \text{ g C m}^{-2} \text{ day}^{-1}$ , Figure 1, i.e., days during which the magnitude of GPP is larger than ER). Following this definition, there may be multiple periods across the course of a calendar year that may have net C uptake; these are added for the calculation of CUP on an annual basis. The MCU

is defined as the maximum value of daily net C uptake of the filtered time series (Figure 1).  $\alpha$  is the ratio of actual carbon sink and hypothetical maximum carbon sink in a year defined as the simple product of  $CUP \times MCU$ , and  $\beta$  is the ratio of actual carbon source and hypothetical maximum carbon source (Figure 1), that is, the length of the calendar year ( $n$ ) minus CUP, multiplied by MCR. We differentiate between indicators calculated from the eddy covariance databases ( $_{sites}$ ) and FLUXCOM ( $_{FLUXCOM}$ ) and explore similarities between them.

## 2.3 | Calculation of the IAV of NEE and relative contributions

Annual NEE can be expressed as a function of the five indicators  $\alpha$ , MCU, CUP,  $\beta$ , and MCR (Figure 1):

$$NEE = \alpha \times MCU \times CUP + \beta \times (n - CUP) \times MCR \quad (1)$$

where  $n = 365$  or  $366$  days. We used a perturbation analysis to separate the contributions of the five indicators to the IAV of NEE and test the sensitivity of this method against a variance decomposition approach in Supporting Information (Text S1). The total differential form of annual NEE with respect to the five indicators is as follows:

$$dNEE = \frac{\partial NEE}{\partial \alpha} d\alpha + \frac{\partial NEE}{\partial MCU} dMCU + \frac{\partial NEE}{\partial CUP} dCUP + \frac{\partial NEE}{\partial \beta} d\beta + \frac{\partial NEE}{\partial MCR} dMCR \quad (2)$$

where

$$\frac{\partial NEE}{\partial \alpha} = MCU \times CUP$$

$$\frac{\partial NEE}{\partial MCU} = \alpha \times CUP$$

$$\frac{\partial NEE}{\partial CUP} = \alpha \times MCU - \beta \times MCR$$

$$\frac{\partial NEE}{\partial \beta} = -MCR \times (CUP - n)$$

$$\frac{\partial NEE}{\partial MCR} = -\beta \times (CUP - n)$$

and higher order terms are excluded. Equation (2) explains more than 97% of the variability of observed NEE across all ecosystems on average.

In practice, the differentials of annual NEE and of the five indicators are approximated by the anomalies ( $\Delta$ ) of the variables, namely, the differences between the variables with respect to their long-term mean values. The annual NEE anomaly is separated into five independent components, that is,  $\frac{\partial NEE}{\partial \alpha} d\alpha$ ,  $\frac{\partial NEE}{\partial MCU} dMCU$ ,  $\frac{\partial NEE}{\partial CUP} dCUP$ ,  $\frac{\partial NEE}{\partial \beta} d\beta$ ,  $\frac{\partial NEE}{\partial MCR} dMCR$  representing the annual NEE change induced by the five indicators, respectively. The relative contributions of the changes in the five indicators to the IAV of NEE were calculated as Equation (3) according to the consistency of

$\frac{\partial \text{NEE}}{\partial \alpha} d\alpha$ ,  $\frac{\partial \text{NEE}}{\partial \text{MCU}} d\text{MCU}$ ,  $\frac{\partial \text{NEE}}{\partial \text{CUP}} d\text{CUP}$ ,  $\frac{\partial \text{NEE}}{\partial \beta} d\beta$ ,  $\frac{\partial \text{NEE}}{\partial \text{MCR}} d\text{MCR}$  with annual NEE anomaly over the period 1980–2013 (Ahlström et al., 2015; Zhou et al., 2017).

$$\xi_x = \frac{\sum_i \frac{\partial \text{NEE}}{\partial x} dx_i \frac{|\Delta \text{NEE}_i|}{\Delta \text{NEE}_i}}{\sum_i |\Delta \text{NEE}_i|}, \quad (3)$$

where  $i$  refers to the year from 1980 to 2013;  $x$  represents the  $\alpha$ , MCU, CUP,  $\beta$ , or MCR, and  $\Delta \text{NEE}_i$  is the annual NEE anomaly based on Equation (2).  $\xi_x$  represents the relative contributions of the five indicators to the IAV of NEE. In Equation (3), the positive sign reveals identical IAV of the indicator with annual NEE, and vice versa, and the magnitude denotes the amount of the relative contribution.

### 3 | RESULTS

#### 3.1 | Spatial patterns of mean $\alpha$ , MCU, CUP, $\beta$ , MCR, and their IAV

Global patterns of  $\alpha$ , MCU, CUP,  $\beta$ , and MCR from the eddy covariance observations and FLUXCOM products were similar. Ecosystems with high mean negative NEE (i.e., strong carbon sinks) had large  $\alpha$  and CUP; for example, the largest mean  $\alpha$  ( $\alpha_{\text{FLUXCOM}} = 0.75$ ,  $\alpha_{\text{sites}} = 0.61$ , Figure 2a,b) and CUP ( $\text{CUP}_{\text{FLUXCOM}} = 365.25$  days,  $\alpha_{\text{sites}} = 365.25$  days, Figure 1d) were found in tropical rainforests; while  $\alpha$  and CUP average about 0.45 ( $\alpha_{\text{sites}} = 0.44 \pm 0.08$ ,  $\alpha_{\text{FLUXCOM}} = 0.48 \pm 0.10$ ) and 180 days ( $\text{CUP}_{\text{sites}} = 178 \pm 68$ ,  $\text{CUP}_{\text{FLUXCOM}} = 187 \pm 94$  days), respectively, in boreal and temperate ecosystems (Figure 2b,d). Mean MCU was greater in forests ( $\text{MCU}_{\text{sites}} = -5.73 \pm 2.52$ ,  $\text{MCU}_{\text{FLUXCOM}} = -2.99 \pm 0.99$  g C m<sup>-2</sup> day<sup>-1</sup>) than in other ecosystems ( $\text{MCU}_{\text{sites}} = -5.38 \pm 3.32$ ,  $\text{MCU}_{\text{FLUXCOM}} = -1.62 \pm 1.14$  g C m<sup>-2</sup> day<sup>-1</sup>, Figure 2c) noting the convention that net C uptake by the land surface is denoted as negative. Mean  $\beta$  and MCR had relatively low spatial variability across the globe (Figure 2e,f). Mean  $\beta$  ( $\beta_{\text{sites}} = 0.39 \pm 0.08$ ,  $\beta_{\text{FLUXCOM}} = 0.52 \pm 0.12$ , Figure 2e) was about 0.4 but MCR from FLUXCOM was smaller than that of tower observations ( $\text{MCR}_{\text{sites}} = 2.37 \pm 1.34$ ,  $\text{MCR}_{\text{FLUXCOM}} = 0.40 \pm 0.19$  g C m<sup>-2</sup> day<sup>-1</sup>, Figure 2f).

We found hot spots of NEE IAV in eastern and southern South America, eastern and southern Africa, Southeast Asia, Australia, central and eastern North America, and Europe (Figure 2g). Although the IAV in  $\alpha$ , MCU, CUP,  $\beta$ , and MCR created the IAV of NEE, the MCU and CUP had larger IAV than  $\alpha$ ,  $\beta$ , and MCR at the global scale (Figure 2h–l). The larger IAV of MCU was mainly distributed in boreal and temperate ecosystems while the larger IAV of CUP was focused on water-limited ecosystems (Figure 2i,j).

#### 3.2 | Relative contributions of $\alpha$ , MCU, CUP, $\beta$ , and MCR to the IAV of NEE

The relative contributions of these five indicators to the IAV of NEE were different for different ecosystems, climate zones, and vegetation types (Figures 3 and 4). Eddy covariance observations and FLUXCOM products consistently showed that the IAV of MCU and

CUP contributed more to the IAV of NEE than that of  $\alpha$ ,  $\beta$ , and MCR at the global scale (Figure 3 and S2), especially across boreal, temperate, and tropical ecosystems for the case of MCU and water-limited ecosystems for the case of CUP (Figure 3b,c). The IAV of  $\alpha$  contributed nearly 40% to the IAV of NEE in tropical forests (Figure 3a). The IAV of MCU contributed about 60% of the IAV of NEE across different latitude bands (30–60°N, 5°S–5°N, and 40–60°S), while the IAV of CUP played a dominant role between 10 and 30°S (40%, Figure 3f). The contributions of  $\alpha$ , MCU, and CUP to the IAV of NEE were roughly equal across 20°N (Figure 3f) in the humid subtropical climate zone that still experiences seasonality in CUP. The contributions of  $\beta$  and MCR to the IAV of NEE were small (<10%) and relatively stable across latitudes.

Across different vegetation types, the contributions of  $\alpha$ , MCU, CUP,  $\beta$ , and MCR from the eddy covariance observations and FLUXCOM products were similar.  $\alpha$  contributed about 40% of the IAV of NEE in EBF (FLUXCOM: 38%, Sites: 41%, see Figure 4 for a list of abbreviations), but less than 20% in all other vegetation types (Figure 4a). The contribution of MCU to the IAV of NEE in forests (EBF, DBF, ENF, DNF, FLUXCOM: 60%–67%, Sites: 40%–50%) was larger than that of nonforests (GRA, SHR, CRO, SAV, FLUXCOM: 39%–47%, Sites: 20%–50%). Conversely, the contribution of CUP to the IAV of NEE in nonforested ecosystems (FLUXCOM: 30%–32%, Sites: 37%–66%) contributed more than that of forests (FLUXCOM: 12%–19%, Sites: 13%–38%, Figure 4). The contributions from  $\beta$  (<4%) and MCR (5%–20%) were smaller and less variable among different vegetation types (Figure 4d,e). In summary, CUP played a dominant role in controlling the IAV of NEE in water-limited systems (Figure 5) while MCU contributed more in temperature and radiation-limited ecosystems (i.e., energy-limited ecosystems; Nemani et al., 2003).

#### 3.3 | Model comparison

The relative contributions of MCU and CUP to the IAV of NEE calculated from LPJ and MStMIP models mismatched that of FLUXCOM observations (Figures 6 and 7). Results from LPJ showed that the IAV of  $\alpha$ , MCU, CUP,  $\beta$ , and MCR explained 6%, 29%, 51%, 3%, and 12% the IAV of NEE, respectively (Figure 6f–j), which were similar to that of the MStMIP models (9%, 30%, 49%, 2%, and 9%, respectively, Figure 6k–o), but FLUXCOM observations found their relative contributions to the IAV of NEE to be 14%, 48%, 25%, 2%, and 8%, respectively (Figure 6a–e). Although both the LPJ model and MStMIP outputs showed MCU and CUP dominated the IAV of NEE at global scale, the contribution of MCU to the IAV of NEE from land surface models was underestimated to about 18% (Figure 6b,g,i), while the contribution of CUP was overestimated to about 25% (Figure 6c,h,m). The main areas for the mismatch between land surface models and observations were in forest, rather than nonforests ecosystems (Figure 7). Models underestimated the contribution of MCU in evergreen broadleaf forests, deciduous broadleaf forests, and evergreen needleleaf forests (Figure 7a) while the contribution of CUP was largely overestimated in these vegetation types (Figure 7b).



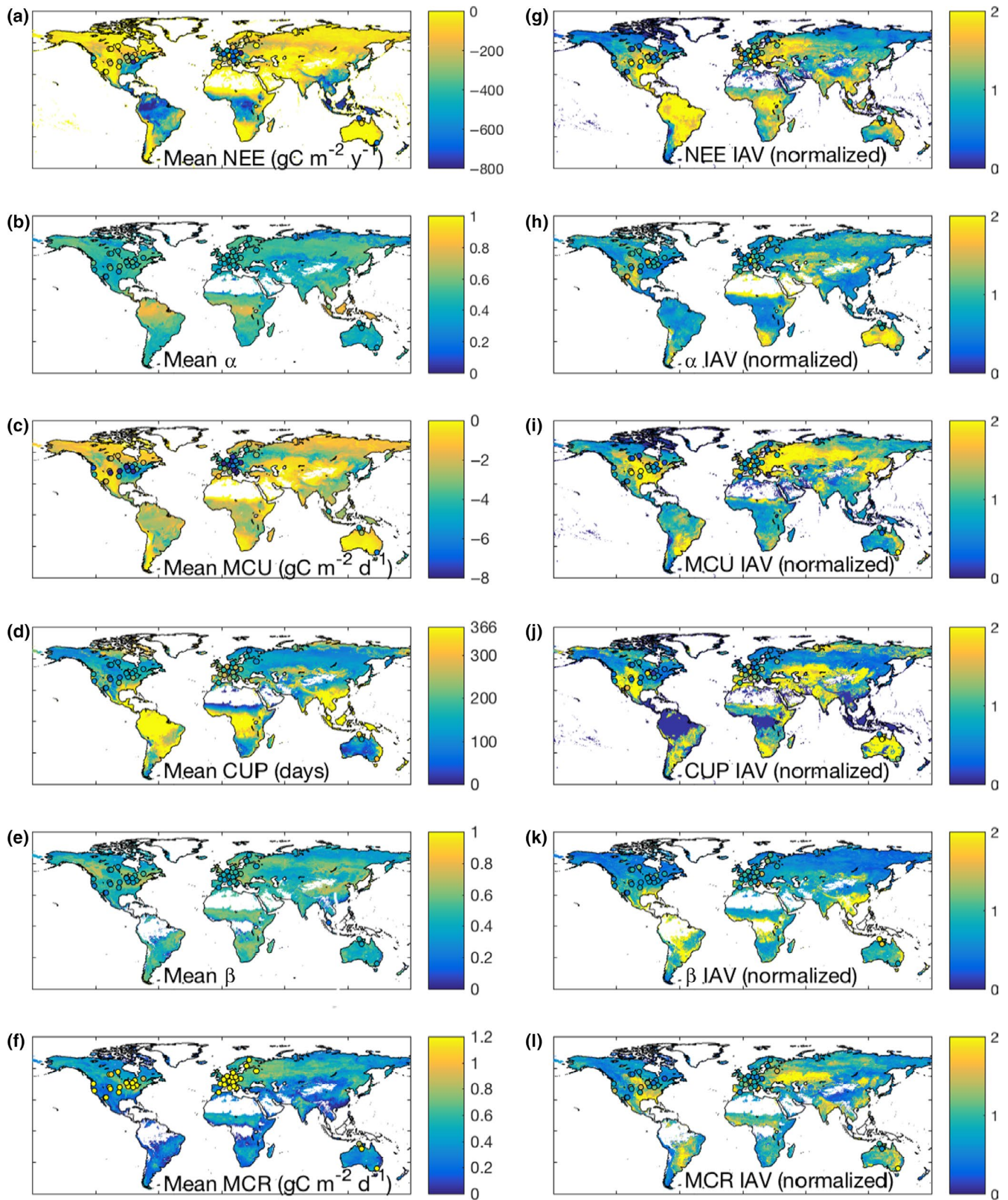


**FIGURE 2** Global patterns of mean net ecosystem CO<sub>2</sub> exchange (NEE),  $\alpha$ , maximum carbon uptake (MCU), carbon uptake period (CUP),  $\beta$ , maximum carbon release (MCR), and their interannual variability (IAV). Global patterns of mean NEE (a),  $\alpha$  (b), MCU (c), CUP (d),  $\beta$  (e), and MCR (f) using FLUXCOM (median from three products, 1980–2013) and eddy covariance research sites (circles). Global patterns of the IAV of NEE (g),  $\alpha$  (h), MCU (i), CUP (j),  $\beta$  (k), and MCR (l) using FLUXCOM (median from three products). The magnitude of IAV (right) is defined as standard deviation of annual value normalized by the mean standard deviation (values above 1 indicate above-average IAV) [Colour figure can be viewed at [wileyonlinelibrary.com](http://wileyonlinelibrary.com)]

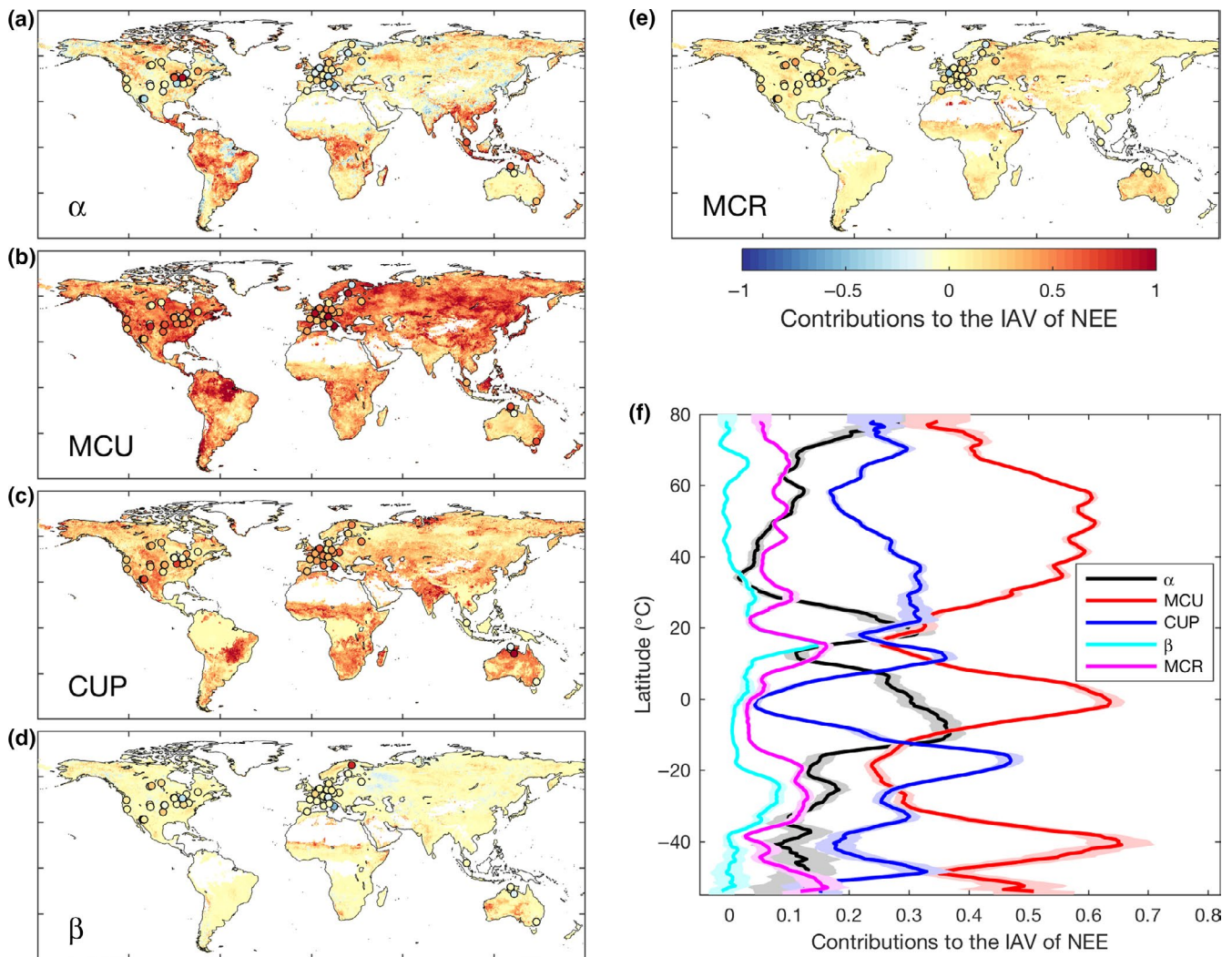


**FIGURE 3** The relative contributions of (a)  $\alpha$ , (b) MCU, (c) CUP, (d)  $\beta$ , and (e) MCR to the interannual variability of net ecosystem CO<sub>2</sub> exchange (NEE) and their latitudinal patterns ( $\pm$ standard error, f) using the median of three FLUXCOM products and eddy covariance research sites (circles). The same results using a variance decomposition method are presented in Figure S2 [Colour figure can be viewed at [wileyonlinelibrary.com](http://wileyonlinelibrary.com)]

## 4 | DISCUSSION

### 4.1 | An integrated approach for quantifying the IAV of NEE

This study sheds new light on the IAV of terrestrial carbon exchange at global scale as revealed by eddy-flux measurements of NEE and FLUXCOM NEE products. We have conceptualized the seasonal pattern of NEE into its observed MCU and release, the CUP, and two parameters,  $\alpha$  and  $\beta$ , that describe the actual carbon sink and source versus hypothetical maximum carbon sink and source defined by other parameters (Figure 1). IAV in  $\alpha$ , MCU, CUP,  $\beta$ , and MCR create the IAV of NEE. The new approach demonstrated in this study is suitable for all ecosystems globally, including dryland, Mediterranean, and tropical ecosystems. Xia et al. (2015) and Zhou et al. (2016) reported that the decomposing method of GPP works well for the ecosystems with distinct one-peak seasonal

patterns, however, its explanatory power is very limited in dryland, Mediterranean, and tropical ecosystems that not exhibit a single seasonal C uptake signal. Our study complements this knowledge gap and provides new insight into the IAV of NEE globally.

The IAV of NEE is explained by indicators that are related to underlying biological processes, for example, physiology and phenology, which can help diagnose causes of its interannual variation. Controls of IAV of NEE are complex because NEE is comprised of two separate fluxes, GPP and ER, driven by different factors including light, temperature, soil moisture, and leaf area index, whose impact and control will differ by ecosystem, climate space, season, and more (Baldocchi, Chu, & Reichstein, 2018; Baldocchi, Ryu, & Keenan, 2016; Zeng, Mariotti, & Wetzel, 2005). These five indicators related to phenology and physiology provide a simple way to track the variations of NEE. Environmental drivers may ultimately cause the IAV of NEE by regulating these phenological and physiological indicators



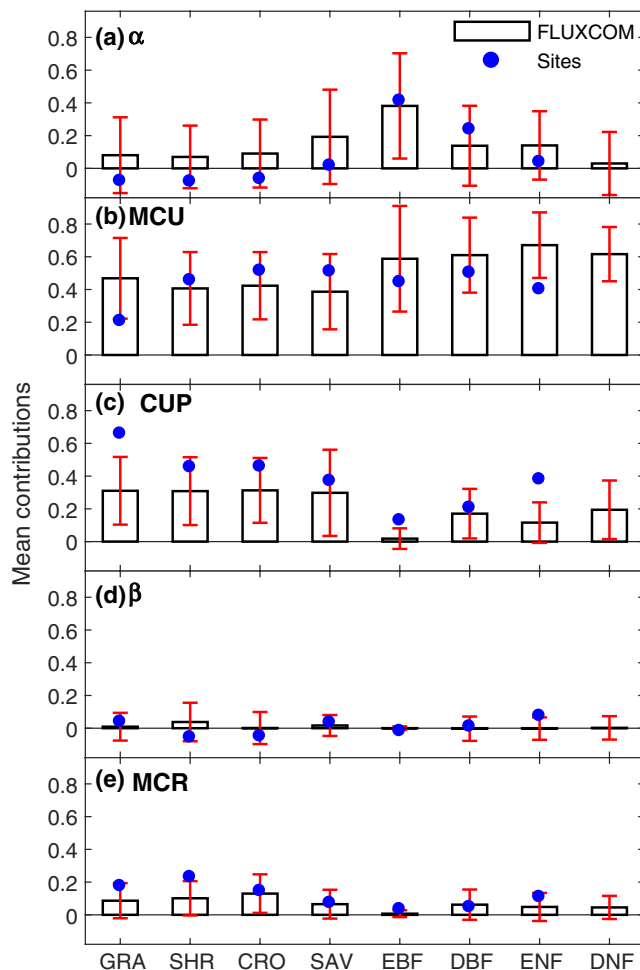


**FIGURE 4** Mean contributions ( $\pm$ standard deviation) of (a)  $\alpha$ , (b) MCU, (c) CUP, (d)  $\beta$ , and (e) MCR to the interannual variability of net ecosystem  $\text{CO}_2$  exchange using FLUXCOM and tower sites across different vegetation types. CRO, croplands; DBF, deciduous broadleaf forests; DNF, deciduous needleleaf forests; EBF, evergreen broadleaf forests; ENF, evergreen needleleaf forests; GRA, grasslands; SAV, savannas; SHR, shrublands [Colour figure can be viewed at [wileyonlinelibrary.com](http://wileyonlinelibrary.com)]

(Fu, Stoy, et al., 2017; Niu et al., 2017). Thus, understanding the relationships between climate and these phenological and physiological indicators could reveal fundamental mechanisms underlying IAV of NEE and be useful for better predicting annual NEE under global change. Additionally, we found that mean  $\alpha$  increased from boreal and temperate ecosystems (0.4) to tropical ecosystems (0.75), which is critical for understanding global patterns of NEE because  $\alpha$  characterizes the capacity of terrestrial ecosystem productivity and shapes the seasonality of NEE. If the daily NEE always equals the MCU during the growing season, the  $\alpha$  will be equal to 1. But this never happens because the environmental conditions are changing and are not always ideal. In this way,  $\alpha$  reflects how much C uptake is constrained by environmental drivers during the growing season.

Mean MCU and MCR from FLUXCOM were lower than that observed at the site level, due in part to the spatial averaging of the MCU and MCR by FLUXCOM that dampens their mean values and uncertainties that

arise from the upscaling method (Jung et al., 2011; Tramontana et al., 2016). It has to be considered that the FLUXCOM product is driven by data from flux networks that are limited in some areas (e.g., the tropics and the Southern Hemisphere); therefore, these observation-driven estimates are underconstrained in those areas. A second reason for the discrepancy could be the difference of studied period, which is from 1980 to 2013 for FLUXCOM, while site observations only cover 5–15 years.

## 4.2 | Dominant role of MCU in contributing to the IAV of NEE

This study establishes that the IAV of global NEE is largely explained by the physiological (MCU) and phenological indicators (CUP), especially the former. Perhaps surprisingly,  $\alpha$  controls only about 10% of the IAV in NEE in the temperate and boreal zones. In other words, the ratio of actual to hypothetical maximum C sink is less variable than the size of the “box” described by CUP and MCU that defines it. The small contributions of  $\beta$  and MCR to the IAV of NEE are fairly constant across the globe, indicating that the IAV of NEE is driven by the net  $\text{CO}_2$  uptake during the growing season, rather than net  $\text{CO}_2$  release during the nongrowing season. A small relative change in MCU is often indicative of substantial changes in peak NEE and thus annual net C uptake (Fu, Dong, et al., 2017; Fu, Stoy, et al., 2017; Zscheischler et al., 2016). The important role of MCU to NEE also has been recognized in a number of recent studies on changes to the terrestrial carbon cycle (Gonsamo, Chen, & Ooi, 2018; Reichstein, Bahn, Mahecha, Kattge, & Baldocchi, 2014; Zhou et al., 2017; Zscheischler et al., 2016). Specifically, the numbers of occurrences of high values in observed daily ecosystem fluxes are strongly correlated with their annual sums, while the influence of phenological transitions has less importance (Zscheischler et al., 2016). It was also well documented that annual NEE correlates well with the maximum light saturated GPP at seven European long-term observation sites (Reichstein et al., 2014). Here, we demonstrated that MCU also dominates the IAV of NEE at global scale, especially in temperature- and radiation-limited ecosystems (Figure 5). These results suggest that variations of  $\text{CO}_2$  uptake during the peak growing season are critical in determining the interannual variation of ecosystem C cycle and its responses to the changing climate.

Not only does MCU dominate the IAV of NEE at the global scale, but there is also an increasing trend in MCU which contributes to the increasing trend in C sink strength (Fu, Dong, et al., 2017). Gonsamo et al. (2018) reported that the peak season plant activity (peak maximum NDVI value) increased by 7.8% for 1982–2015, which further highlights the importance of MCU in contributing the land C sink. The increasing trends in summertime C uptake in northern ecosystems (Graven et al., 2013) have been attributed to increasing leaf area and plant biomass (Myneni, Keeling, Tucker, Asrar, & Nemani, 1997; Pan et al., 2011), increasing coverage of evergreen shrubs and trees (Walther et al., 2002), and shifting the age composition toward fast growing vegetation after disturbances that have more intense seasonal C uptake (Soja et al., 2007), all suggesting ongoing changes in MCU that must be further studied to understand the variability of the global C cycle.



**FIGURE 5** Frequency distributions of the contribution of CUP (a) and MCU (b) to the interannual variability of net ecosystem  $\text{CO}_2$  exchange across global regions in which the net primary productivity is limited by water, temperature, or radiation [Colour figure can be viewed at [wileyonlinelibrary.com](http://wileyonlinelibrary.com)]

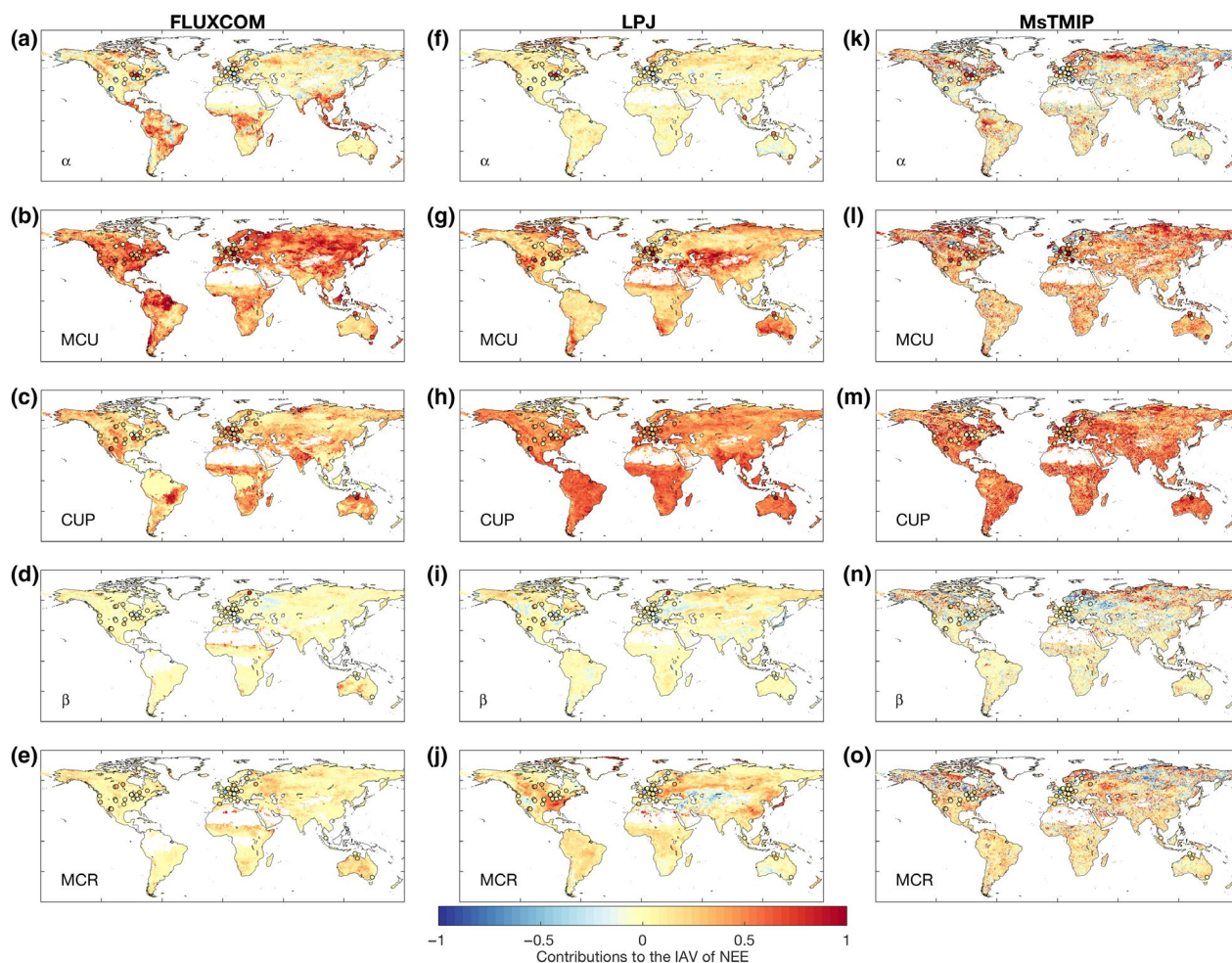
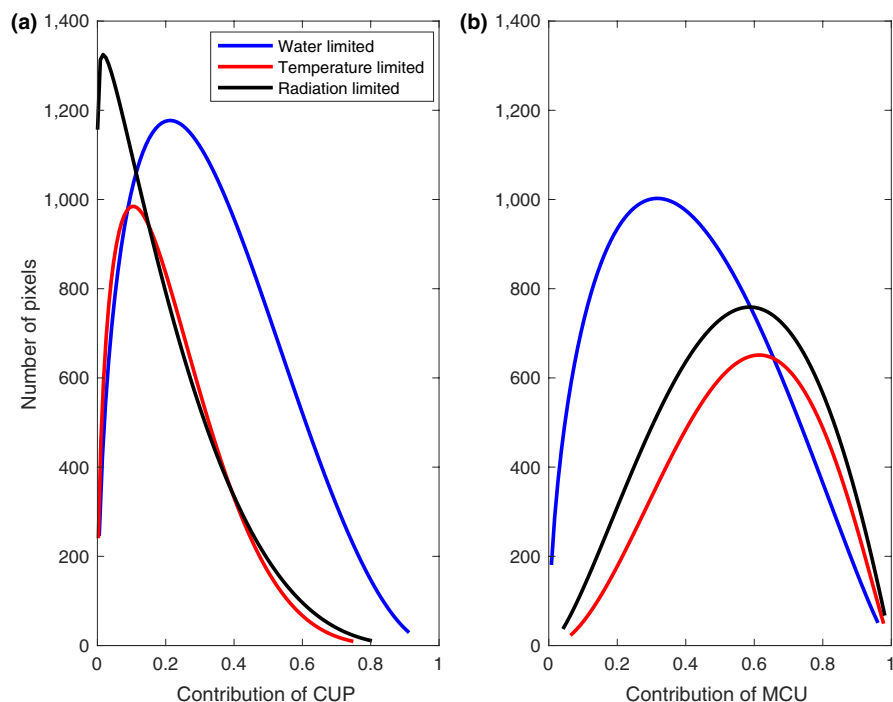


**FIGURE 6** The relative contributions of  $\alpha$ , maximum carbon uptake (MCU), carbon uptake period (CUP),  $\beta$ , maximum carbon release (MCR) to the interannual variability of net ecosystem  $\text{CO}_2$  exchange using FLUXCOM (a–e), Lund-Potsdam-Jena (LPJ) (f–j), Multi-scale Synthesis and Terrestrial Model Inter-comparison Project (MsTMIP) models (k–o), and eddy covariance research sites (circles) [Colour figure can be viewed at [wileyonlinelibrary.com](http://wileyonlinelibrary.com)]

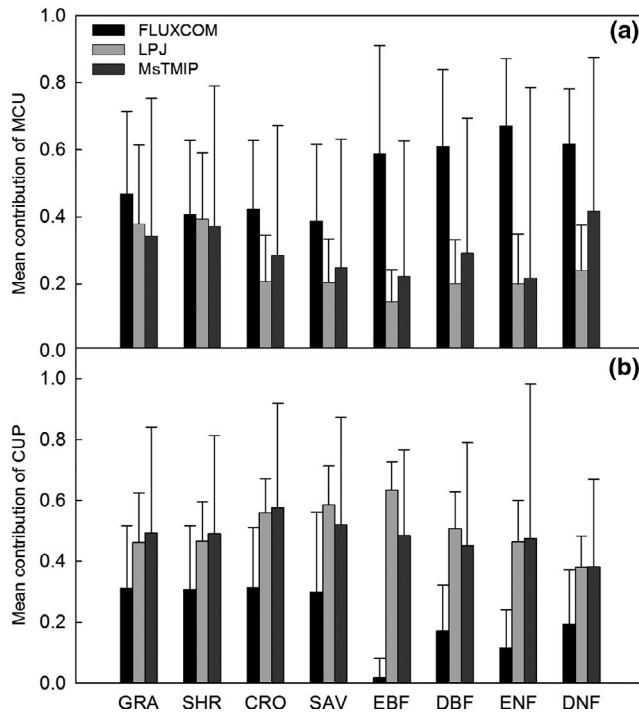


**FIGURE 7** Mean contributions ( $\pm$ standard deviation) of the interannual variability (IAV) of maximum carbon uptake (MCU, a) and carbon uptake period (CUP, b) to the IAV of net ecosystem  $\text{CO}_2$  exchange using FLUXCOM observations, Lund-Potsdam-Jena (LPJ), and Multi-scale Synthesis and Terrestrial Model Inter-comparison Project (MsTMIP) outputs across different vegetation types. CRO, croplands; DBF, deciduous broadleaf forests; DNF, deciduous needleleaf forests; EBF, evergreen broadleaf forests; ENF, evergreen needleleaf forests; GRA, grasslands; SAV, savannas; SHR, shrublands

In water-limited ecosystems, however, we found that CUP played an important role in contributing to the IAV of NEE. In water-limited ecosystems, changes in CUP—often due to precipitation events—may appreciably change annual C uptake (Ahlström et al., 2015; Poulter et al., 2014). Although the length of CUP in water-limited ecosystems is shorter than that of temperature- or radiation-limited ecosystems (Figure 2d), the IAV of CUP in water-limited ecosystems is larger (Figure 2j), and dominates the IAV of NEE. Plants living in water-limited areas often opportunistically respond to rainfall events, which thereby determine productivity (Tang, Arnone III, Verburg, Jasoni, & Sun, 2015). Many recent studies have advanced our knowledge of how ecosystem phenology—and thereby CUP—influences the terrestrial ecosystem C cycle (Buermann et al., 2018; Churkina et al., 2005; Piao, Friedlingstein, Ciais, Viovy, & Demarty, 2007; Richardson et al., 2013), and our results further emphasize its importance for understanding the IAV of NEE in water-limited ecosystems.

### 4.3 | Land surface models cannot capture the contributions of MCU and CUP

Compared with the relative contributions of MCU and CUP to the IAV of NEE calculated from FLUXCOM, both the LPJ model and MsTMIP models underestimated the contribution of MCU to the IAV

of NEE and overestimated the contribution of CUP. The main areas for the mismatch between land surface models and observations were in forests, rather than nonforests ecosystems (Figures 6 and 7). The mean and IAV of the MCU in forests are larger than that of nonforests ecosystems, and the land surface models do not capture this large IAV of MCU in forests, leading to the underestimation of its contribution to the IAV of NEE. Our results suggested that future research needs to improve the simulating capability of MCU, especially in forests, for land surface models. In addition to model structure, particular attention to the meteorological data being used and how this affects uncertainty in daily fluxes should be further investigated.

The underestimation of MCU's contribution to the IAV of NEE in land surface models might be caused by an underestimation of the maximum leaf area index, plant photosynthetic capacity, and/or missing representation of agricultural management. Many land surface models underestimate the maximum leaf area index, especially in the high latitudes (Winkler, Myneni, Alexandrov, & Brovkin, 2019), which leads to an underestimation of GPP. Huang et al. (2018) also reported the uncertainty of simulating the plant photosynthetic capacity in land surface models. For example, the control of leaf nitrogen concentrations and environmental variables (e.g., temperature, radiation, day length, and humidity) are conventionally assumed to be constant for each plant functional type or to vary linearly with leaf nitrogen concentrations in current terrestrial biosphere models, when modeling plant photosynthetic capacity (e.g.,  $V_{\text{cmax}}$ ; Ali et al., 2015). Moreover, models differ in the design of crop types and the ways in which they deal with crop and agricultural management. MsTMIP models might underestimate the contribution of agricultural activities to the MCU, because most models do not explicitly represent crops and agricultural management (Huang et al., 2018; Thomas et al., 2016). In addition, most models underestimate the magnitude of heterotrophic respiration (Liu et al., 2018). It is difficult to capture the complexity of heterotrophic respiration (e.g., microbial responses; Mäkiranta et al., 2009), which impacts ecosystem respiration and thus on MCU and CUP. Dynamic Global Vegetation models have routinely incorporated temperature and moisture constraints on heterotrophic respiration, but the effects of moisture on decomposition rate are much more uncertain than temperature (Koven, Hugelius, Lawrence, & Wieder, 2017; Sierra, Trumbore, Davidson, Vicca, & Janssens, 2015).

### 4.4 | Implications of MCU and CUP under changing climate

The predominant role of peak growing season physiology in causing the IAV in the terrestrial carbon cycle has important implications for understanding the global C cycle in response to climate change. Because climate change likely results in an increased frequency and intensity of summer drought and heat waves (Ciais et al., 2005; Hall, Qu, & Neelin, 2008; Sheffield & Wood, 2008), future changes in growing season climate may cause substantial changes in C cycling by impacting the  $\text{CO}_2$  uptake capacity at peak

growing season, which would lead to larger IAV in the terrestrial C cycle and atmospheric CO<sub>2</sub> growth rates. To better simulate land CO<sub>2</sub> exchange under changing climate, it is urgent for global models to realistically represent physiological processes that determine peak growing season ecosystem function. The latter are highly dynamic and may require dynamic instead of fixed parameter values for the maximum rate of carboxylation in models to accurately simulate the variability of MCU (Li et al., 2016; Xiao, Davis, Urban, & Keller, 2014).

Previous work on the IAV of NEE mostly has focused on the ultimate causes of climate impacts (Jung et al., 2017; Poulter et al., 2014; Wang et al., 2014; Zeng et al., 2005). Climate causes the IAV of NEE largely through its influence on MCU and CUP. Numerous studies have attributed the IAV of terrestrial C cycle to different climate factors with generally conflicting results (Kindermann, Würth, Kohlmaier, & Badeck, 1996; Schaefer et al., 2002; Zeng et al., 2005), and few have explicitly examined how climate factors impact the fundamental processes of terrestrial C cycle and consequently cause the IAV of C uptake. As revealed in this study, the processes underlying the IAV in NEE are primarily physiological and phenological, which are associated with MCU and CUP, both of which are regulated by changes in environmental factors, but in different ways. If these climate factors have compensatory effects on MCU and CUP, they will lead to negligible impacts on annual NEE (Buermann et al., 2018; Fu, Stoy, et al., 2017; Wolf et al., 2016). For example, a warmer spring usually induces a longer growing season and thus results in higher production. But a subsequent warmer and drier summer may suppress summer production, potentially offsetting the increase in terrestrial ecosystem production that is expected with a longer growing season (Angert et al., 2005; Cleland, Chuine, Menzel, Mooney, & Schwartz, 2007). Namely, in some ecosystems, early spring and longer growing seasons may decrease annual GPP or NEE because the earlier onset of growing season may increase transpiration, leaving less available water in the soil in summer and limiting plant growth later in the growing season (Kljun et al., 2006; Wolf et al., 2016). Such offsetting and compensatory impacts of climate factors could be reasons why different studies in the past have generated contradictory or conflicting results on the causes of the IAV in terrestrial C fluxes and atmospheric CO<sub>2</sub> growth rate. Future research needs to pay more attention to the different effects of climate anomalies on the MCU and CUP for a better understanding of the IAV of NEE globally, as well as exploring how elevated atmospheric CO<sub>2</sub> interacts with leaf and canopy processes.

In summary, this study demonstrated a universal approach for integrating phenology and physiology globally and sheds new light on explaining IAV in terrestrial carbon exchange at global scale. It suggests that the IAV in terrestrial NEE can be understood by decomposing it into proximate causes of C uptake using metrics of phenology and physiology. The IAV of NEE was determined predominately by variability in the MCU at the global scale, which explained 48% of the IAV of NEE on average. CUP played an important

role in contributing to the IAV of NEE in water-limited ecosystems while MCU dominated the IAV of NEE in temperature- and radiation-limited ecosystems. The LPJ model and the MSTMIP models underestimate the contribution of MCU to the IAV of NEE by about 18% on average, and overestimate the contribution of CUP by about 25%. The major role of MCU in determining the IAV in NEE is supported by recent advances in terms of the global increase of seasonal amplitude of atmosphere CO<sub>2</sub> concentration (Graven et al., 2013), increasing greenness in northern ecosystems (Myneni et al., 1997), and increasing trends in annual CO<sub>2</sub> uptake in temperate and boreal areas (Keenan et al., 2014). This study provides a new perspective on the proximate causes of the IAV in NEE, which may explain the different results in previous studies on the ultimate causes of IAV in the C cycle (Kindermann et al., 1996; Poulter et al., 2014; Schaefer et al., 2002; Wang et al., 2014; Zeng et al., 2005). The mechanisms underlying the IAV in the terrestrial C cycle through changes in CO<sub>2</sub> uptake amplitude and period is of critical importance for improving our ability to project future change in the earth system.

## ACKNOWLEDGEMENTS

We would like to thank Dr. Ramakrishna Nemani and Dr. Hirofumi Hashimoto for providing the datasets for climatic constraints to plant growth, and Dr. Martin Jung for valuable comments. This work was financially supported by the National Key R & D Program of China (2018YFA0606102), National Natural Science Foundation of China (31625006), and the international collaboration project of Chinese Academy of Sciences (131A11KYSB20180010). Z. Z and B. P. were funded by the Gordon and Betty Moore Foundation through Grant GBMF5439. BP acknowledges support through the NASA Terrestrial Ecology Program. PCS acknowledges contributions from the U S National Science Foundation awards DEB 1552976, OIA 1632810, and EF 1702029 and the USDA-NIFA Hatch project 228396. This work used eddy covariance data acquired and shared by the FLUXNET community, including these networks: AmeriFlux, AfriFlux, AsiaFlux, CarboAfrica, CarboEuropeIP, CarboItaly, CarboMont, ChinaFlux, Fluxnet-Canada, GreenGrass, ICOS, KoFlux, LBA, NECC, OzFlux-TERN, TCOS-Siberia, and USCCC. The ERA-Interim reanalysis data are provided by ECMWF and processed by LSCE. The FLUXNET eddy covariance data processing and harmonization was carried out by the European Fluxes Database Cluster, AmeriFlux Management Project, and Fluxdata project of FLUXNET, with the support of CDIAC and ICOS Ecosystem Thematic Center, and the OzFlux, ChinaFlux, and AsiaFlux offices.

## DATA AVAILABILITY STATEMENT

All the datasets used for this analysis are available for download via the following links. Eddy-covariance data are from FLUXNET2015 dataset (<http://fluxnet.fluxdata.org/data/fluxnet2015-dataset/>). Three FLUXCOM global products derived from FLUXNET observations by

three machine learning algorithms are from Max Planck Institute for Biogeochemistry (<http://www.fluxcom.org/Products/>). MSTMIP outputs are from NASA Carbon Monitoring System project ([https://daac.ornl.gov/cgi-bin/dsvviewer.pl?ds\\_xmlid=1315](https://daac.ornl.gov/cgi-bin/dsvviewer.pl?ds_xmlid=1315)). Global maps of temperature, water, and radiation constraints to plant growth derived from long-term climate statistics are from Nemani et al. (2003). The MODIS MCD12C1 land-cover product is obtained from Land Processes Distributed Active Archive Center (<https://lpdaac.usgs.gov>).

## ORCID

Zheng Fu  <https://orcid.org/0000-0001-7627-8824>

Paul C. Stoy  <https://orcid.org/0000-0002-6053-6232>

Benjamin Poulter  <https://orcid.org/0000-0002-9493-8600>

Tobias Gerken  <https://orcid.org/0000-0001-5617-186X>

Zhen Zhang  <https://orcid.org/0000-0003-0899-1139>

Shuli Niu  <https://orcid.org/0000-0002-2394-2864>

## REFERENCES

- Ahlstrom, A., Raupach, M. R., Schurgers, G., Smith, B., Arneeth, A., Jung, M., ... Zeng, N. (2015). The dominant role of semi-arid ecosystems in the trend and variability of the land CO<sub>2</sub> sink. *Science*, 348, 895–899. <https://doi.org/10.1126/science.aaa1668>
- Ali, A. A., Xu, C., Rogers, A., McDowell, N. G., Medlyn, B. E., Fisher, R. A., ... Wilson, C. J. (2015). Global-scale environmental control of plant photosynthetic capacity. *Ecological Applications*, 25, 2349–2365. <https://doi.org/10.1890/14-2111.1>
- Angert, A., Biraud, S., Bonfils, C., Henning, C. C., Buermann, W., Pinzon, J., ... Fung, I. (2005). Drier summers cancel out the CO<sub>2</sub> uptake enhancement induced by warmer springs. *Proceedings of the National Academy of Sciences of the United States of America*, 102, 10823–10827. <https://doi.org/10.1073/pnas.0501647102>
- Baldocchi, D., Chu, H., & Reichstein, M. (2018). Inter-annual variability of net and gross ecosystem carbon fluxes: A review. *Agricultural and Forest Meteorology*, 249, 520–533. <https://doi.org/10.1016/j.agrfor.2017.05.015>
- Baldocchi, D., Ryu, Y., & Keenan, T. (2016). Terrestrial carbon cycle variability. *F1000Research*, 5, 2371. <https://doi.org/10.12688/f1000research.8962.1>
- Buermann, W., Forkel, M., O'Sullivan, M., Sitch, S., Friedlingstein, P., Haverd, V., ... Richardson, A. D. (2018). Widespread seasonal compensation effects of spring warming on northern plant productivity. *Nature*, 562, 110–114. <https://doi.org/10.1038/s41586-018-0555-7>
- Chapin III, F. S., Matson, P. A., & Vitousek, P. (2011). *Principles of terrestrial ecosystem ecology*. New York, NY: Springer Science & Business Media.
- Chapin, F. S., Woodwell, G. M., Randerson, J. T., Rastetter, E. B., Lovett, G. M., Baldocchi, D. D., ... Schulze, E.-D. (2006). Reconciling carbon-cycle concepts, terminology, and methods. *Ecosystems*, 9, 1041–1050. <https://doi.org/10.1007/s10021-005-0105-7>
- Chu, H., Baldocchi, D. D., John, R., Wolf, S., & Reichstein, M. (2017). Fluxes all of the time? A primer on the temporal representativeness of FLUXNET. *Journal of Geophysical Research: Biogeosciences*, 122, 289–307. <https://doi.org/10.1002/2016JG003576>
- Churkina, G., Schimel, D., Braswell, B. H., & Xiao, X. (2005). Spatial analysis of growing season length control over net ecosystem exchange. *Global Change Biology*, 11, 1777–1787. <https://doi.org/10.1111/j.1365-2486.2005.001012.x>
- Ciais, P. H., Reichstein, M., Viovy, N., Granier, A., Ogée, J., Allard, V., ... Valentini, R. (2005). Europe-wide reduction in primary productivity caused by the heat and drought in 2003. *Nature*, 437, 529–533. <https://doi.org/10.1038/nature03972>
- Cleland, E. E., Chuine, I., Menzel, A., Mooney, H. A., & Schwartz, M. D. (2007). Shifting plant phenology in response to global change. *Trends in Ecology & Evolution*, 22, 357–365. <https://doi.org/10.1016/j.tree.2007.04.003>
- Dragoni, D., Schmid, H. P., Wayson, C. A., Potter, H., Grimmond, C. S. B., & Randolph, J. C. (2011). Evidence of increased net ecosystem productivity associated with a longer vegetated season in a deciduous forest in south-central Indiana, USA. *Global Change Biology*, 17, 886–897. <https://doi.org/10.1111/j.1365-2486.2010.02281.x>
- Friedl, M. A., & Brodley, C. E. (1997). Decision tree classification of land cover from remotely sensed data. *Remote Sensing of Environment*, 61, 399–409. [https://doi.org/10.1016/S0034-4257\(97\)00049-7](https://doi.org/10.1016/S0034-4257(97)00049-7)
- Fu, Z., Dong, J., Zhou, Y., Stoy, P. C., & Niu, S. (2017). Long term trend and interannual variability of land carbon uptake—The attribution and processes. *Environmental Research Letters*, 12, 014018. <https://doi.org/10.1088/1748-9326/aa5685>
- Fu, Z., Stoy, P. C., Luo, Y., Chen, J., Sun, J., Montagnani, L., ... Niu, S. (2017). Climate controls over the net carbon uptake period and amplitude of net ecosystem production in temperate and boreal ecosystems. *Agricultural and Forest Meteorology*, 243, 9–18. <https://doi.org/10.1016/j.agrformet.2017.05.009>
- Gonsamo, A., Chen, J. M., & Ooi, Y. W. (2018). Peak season plant activity shift towards spring is reflected by increasing carbon uptake by extratropical ecosystems. *Global Change Biology*, 24, 2117–2128. <https://doi.org/10.1111/gcb.14001>
- Graven, H. D., Keeling, R. F., Piper, S. C., Patra, P. K., Stephens, B. B., Wofsy, S. C., ... Bent, J. D. (2013). Enhanced seasonal exchange of CO<sub>2</sub> by northern ecosystems since 1960. *Science*, 341, 1085–1089. <https://doi.org/10.1126/science.1239207>
- Hall, A., Qu, X., & Neelin, J. D. (2008). Improving predictions of summer climate change in the United States. *Geophysical Research Letters*, 35. <https://doi.org/10.1029/2007GL032012>
- Huang, K., Xia, J., Wang, Y., Ahlström, A., Chen, J., Cook, R. B., ... Luo, Y. (2018). Enhanced peak growth of global vegetation and its key mechanisms. *Nature Ecology & Evolution*, 2, 1897–1905. <https://doi.org/10.1038/s41559-018-0714-0>
- Huntzinger, D. N., Schwalm, C., Michalak, A. M., Schaefer, K., King, A. W., Wei, Y., ... Zhu, Q. (2013). The North American Carbon Program Multi-Scale Synthesis and Terrestrial Model Intercomparison Project – Part 1: Overview and experimental design. *Geoscientific Model Development*, 6, 2121–2133. <https://doi.org/10.5194/gmd-6-2121-2013>
- Ichii, K., Hashimoto, H., Nemani, R., & White, M. (2005). Modeling the interannual variability and trends in gross and net primary productivity of tropical forests from 1982 to 1999. *Global and Planetary Change*, 48, 274–286. <https://doi.org/10.1016/j.gloplacha.2005.02.005>
- Jung, M., Reichstein, M., Margolis, H. A., Cescatti, A., Richardson, A. D., Arain, M. A., ... Williams, C. (2011). Global patterns of land-atmosphere fluxes of carbon dioxide, latent heat, and sensible heat derived from eddy covariance, satellite, and meteorological observations. *Journal of Geophysical Research Biogeosciences*, 116. <https://doi.org/10.1029/2010JG001566>
- Jung, M., Reichstein, M., Schwalm, C. R., Huntingford, C., Sitch, S., Ahlström, A., ... Zeng, N. (2017). Compensatory water effects link yearly global land CO<sub>2</sub> sink changes to temperature. *Nature*, 541, 516–520. <https://doi.org/10.1038/nature20780>
- Keenan, T. F., Baker, I., Barr, A., Ciais, P., Davis, K., Dietze, M., ... Richardson, A. D. (2012). Terrestrial biosphere model performance for inter-annual



- variability of land-atmosphere CO<sub>2</sub> exchange. *Global Change Biology*, 18, 1971–1987. <https://doi.org/10.1111/j.1365-2486.2012.02678.x>
- Keenan, T. F., Gray, J., Friedl, M. A., Toomey, M., Bohrer, G., Hollinger, D. Y., ... Richardson, A. D. (2014). Net carbon uptake has increased through warming-induced changes in temperate forest phenology. *Nature Climate Change*, 4, 598–604. <https://doi.org/10.1038/nclimate2253>
- Kindermann, J., Würth, G., Kohlmaier, G. H., & Badeck, F. W. (1996). Interannual variation of carbon exchange fluxes in terrestrial ecosystems. *Global Biogeochemical Cycles*, 10, 737–755. <https://doi.org/10.1029/96GB02349>
- Kljun, N., Black, T. A., Griffis, T. J., Barr, A. G., Gaumont-Guay, D., Morgenstern, K., ... Nescic, Z. (2006). Response of net ecosystem productivity of three boreal forest stands to drought. *Ecosystems*, 9, 1128–1144. <https://doi.org/10.1007/s10021-005-0082-x>
- Koven, C. D., Hugelius, G., Lawrence, D. M., & Wieder, W. R. (2017). Higher climatological temperature sensitivity of soil carbon in cold than warm climates. *Nature Climate Change*, 7, 817–822. <https://doi.org/10.1038/nclimate3421>
- Le Quéré, C., Andrew, R. M., Friedlingstein, P., Sitch, S., Pongratz, J., Manning, A. C., ... Zhu, D. (2018). Global carbon budget 2017. *Earth System Science Data*, 10, 405–448. <https://doi.org/10.5194/essd-10-405-2018>
- Li, Q., Xia, J., Shi, Z., Huang, K., Du, Z., Lin, G., & Luo, Y. (2016). Variation of parameters in a Flux-Based Ecosystem Model across 12 sites of terrestrial ecosystems in the conterminous USA. *Ecological Modelling*, 336, 57–69. <https://doi.org/10.1016/j.ecolmodel.2016.05.016>
- Liu, Z., Ballantyne, A. P., Poulter, B., Anderegg, W. R. L., Li, W., Bastos, A., & Ciais, P. (2018). Precipitation thresholds regulate net carbon exchange at the continental scale. *Nature Communications*, 9, 3596. <https://doi.org/10.1038/s41467-018-05948-1>
- Luo, Y., Shi, Z., Lu, X., Xia, J., Liang, J., Jiang, J., ... Wang, Y.-P. (2017). Transient dynamics of terrestrial carbon storage: Mathematical foundation and its applications. *Biogeosciences*, 14, 145–161. <https://doi.org/10.5194/bg-14-145-2017>
- Mäkiranta, P., Laiho, R., Fritze, H., Hytönen, J., Laine, J., & Minkinen, K. (2009). Indirect regulation of heterotrophic peat soil respiration by water level via microbial community structure and temperature sensitivity. *Soil Biology and Biochemistry*, 41, 695–703. <https://doi.org/10.1016/j.soilbio.2009.01.004>
- Marcolla, B., Rödenbeck, C., & Cescatti, A. (2017). Patterns and controls of inter-annual variability in the terrestrial carbon budget. *Biogeosciences*, 14, 3815–3829.
- Myneni, R. B., Keeling, C. D., Tucker, C. J., Asrar, G., & Nemani, R. R. (1997). Increased plant growth in the northern high latitudes from 1981 to 1991. *Nature*, 386, 698–702. <https://doi.org/10.1038/386698a0>
- Nemani, R. R., Keeling, C. D., Hashimoto, H., Jolly, W. M., Piper, S. C., Tucker, C. J., ... Running, S. W. (2003). Climate-driven increases in global terrestrial net primary production from 1982 to 1999. *Science*, 300, 1560–1563. <https://doi.org/10.1126/science.1082750>
- Niu, S., Fu, Z., Luo, Y., Stoy, P. C., Keenan, T. F., Poulter, B., ... Yu, G. (2017). Interannual variability of ecosystem carbon exchange: From observation to prediction. *Global Ecology and Biogeography*, 26, 1225–1237. <https://doi.org/10.1111/geb.12633>
- Oleson, K., Lawrence, D., Bonan, G., Flanner, M. G., Kluzek, E., Lawrence, P. J., ... Zeng, X. (2010). Technical description of version 4.5 of the Community Land Model (CLM). Rep. National Center for Atmospheric Research, Boulder, 266.
- Pan, Y., Birdsey, R. A., Fang, J., Houghton, R., Kauppi, P. E., Kurz, W. A., ... Hayes, D. (2011). A large and persistent carbon sink in the world's forests. *Science*, 333, 988–993. <https://doi.org/10.1126/science.1201609>
- Papale, D., Reichstein, M., Aubinet, M., Canfora, E., Bernhofer, C., Kutsch, W., ... Yakir, D. (2006). Towards a standardized processing of Net Ecosystem Exchange measured with eddy covariance technique: Algorithms and uncertainty estimation. *Biogeosciences*, 3, 571–583. <https://doi.org/10.5194/bg-3-571-2006>
- Piao, S., Friedlingstein, P., Ciais, P., Viovy, N., & Demarty, J. (2007). Growing season extension and its impact on terrestrial carbon cycle in the Northern Hemisphere over the past 2 decades. *Global Biogeochemical Cycles*, 21. <https://doi.org/10.1029/2006GB002888>
- Poulter, B., Frank, D., Ciais, P., Myneni, R. B., Andela, N., Bi, J., ... van der Werf, G. R. (2014). Contribution of semi-arid ecosystems to interannual variability of the global carbon cycle. *Nature*, 509, 600. <https://doi.org/10.1038/nature13376>
- Reichstein, M., Bahn, M., Mahecha, M. D., Kattge, J., & Baldocchi, D. D. (2014). Linking plant and ecosystem functional biogeography. *Proceedings of the National Academy of Sciences of the United States of America*, 111, 13697–13702. <https://doi.org/10.1073/pnas.1216065111>
- Reichstein, M., Falge, E., Baldocchi, D., Papale, D., Aubinet, M., Berbigier, P., ... Valentini, R. (2005). On the separation of net ecosystem exchange into assimilation and ecosystem respiration: Review and improved algorithm. *Global Change Biology*, 11, 1424–1439. <https://doi.org/10.1111/j.1365-2486.2005.001002.x>
- Richardson, A. D., Keenan, T. F., Migliavacca, M., Ryu, Y., Sonnentag, O., & Toomey, M. (2013). Climate change, phenology, and phenological control of vegetation feedbacks to the climate system. *Agricultural and Forest Meteorology*, 169, 156–173. <https://doi.org/10.1016/j.agrformet.2012.09.012>
- Savitzky, A., & Golay, M. J. (1964). Smoothing and differentiation of data by simplified least squares procedures. *Analytical Chemistry*, 36, 1627–1639. <https://doi.org/10.1021/ac60214a047>
- Schaefer, K., Denning, A. S., Suits, N., Kaduk, J., Baker, I., Los, S., Prihodko, L. (2002). Effect of climate on interannual variability of terrestrial CO<sub>2</sub> fluxes. *Global Biogeochemical Cycles*, 16, 49–1–49–12. <https://doi.org/10.1029/2002GB001928>
- Sheffield, J., & Wood, E. F. (2008). Projected changes in drought occurrence under future global warming from multi-model, multi-scenario, IPCC AR4 simulations. *Climate Dynamics*, 31, 79–105. <https://doi.org/10.1007/s00382-007-0340-z>
- Sierra, C. A., Trumbore, S. E., Davidson, E. A., Vicca, S., & Janssens, I. (2015). Sensitivity of decomposition rates of soil organic matter with respect to simultaneous changes in temperature and moisture. *Journal of Advances in Modeling Earth Systems*, 7, 335–356. <https://doi.org/10.1002/2014MS000358>
- Sitch, S., Smith, B., Prentice, I. C., Arneth, A., Bondeau, A., Cramer, W., ... Venevsky, S. (2003). Evaluation of ecosystem dynamics, plant geography and terrestrial carbon cycling in the LPJ dynamic global vegetation model. *Global Change Biology*, 9, 161–185. <https://doi.org/10.1046/j.1365-2486.2003.00569.x>
- Soja, A. J., Tchepakova, N. M., French, N. H. F., Flannigan, M. D., Shugart, H. H., Stocks, B. J., ... Stackhouse, P. W. (2007). Climate-induced boreal forest change: Predictions versus current observations. *Global and Planetary Change*, 56, 274–296. <https://doi.org/10.1016/j.gloplacha.2006.07.028>
- Tang, G., Arnone II, J., Verburg, P., Jasoni, R., & Sun, L. (2015). Trends and climatic sensitivities of vegetation phenology in semiarid and arid ecosystems in the US Great Basin during 1982–2011. *Biogeosciences*, 12, 6985–6997. <https://doi.org/10.5194/bg-12-6985-2015>
- Thomas, R. T., Prentice, I. C., Graven, H., Ciais, P., Fisher, J. B., & Hayes, D. J., ... Zeng, N. (2016). Increased light-use efficiency in northern terrestrial ecosystems indicated by CO<sub>2</sub> and greening observations. *Geophysical Research Letters*, 43, 11339–11349. <https://doi.org/10.1002/2016GL070710>
- Tramontana, G., Jung, M., Camps-Valls, G., Ichii, K., Raduly, B., Reichstein, M., ... Papale, D. (2016). Predicting carbon dioxide and energy fluxes across global FLUXNET sites with regression algorithms. *Biogeosciences Discussions*, 1–33. <https://doi.org/10.5194/bg-2015-661>

- Walther, G.-R., Post, E., Convey, P., Menzel, A., Parmesan, C., Beebee, T. J. C., ... Bairlein, F. (2002). Ecological responses to recent climate change. *Nature*, 416, 389–395. <https://doi.org/10.1038/416389a>
- Wang, X., Piao, S., Ciais, P., Friedlingstein, P., Myneni, R. B., Cox, P., ... Chen, A. (2014). A two-fold increase of carbon cycle sensitivity to tropical temperature variations. *Nature*, 506, 212. <https://doi.org/10.1038/nature12915>
- Wei, Y., Liu, S., Huntzinger, D. N., Michalak, A. M., Viovy, N., Post, W. M., ... Shi, X. (2014). The North American carbon program multi-scale synthesis and terrestrial model intercomparison project—Part 2: Environmental driver data. *Geoscientific Model Development Discussions*, 7, 2875–2893. <https://doi.org/10.5194/gmd-7-2875-2014>
- Winkler, A. J., Myneni, R. B., Alexandrov, G. A., & Brovkin, V. (2019). Earth system models underestimate carbon fixation by plants in the high latitudes. *Nature Communications*, 10, 885. <https://doi.org/10.1038/s41467-019-08633-z>
- Wolf, S., Keenan, T. F., Fisher, J. B., Baldocchi, D. D., Desai, A. R., Richardson, A. D., ... van der Laan-Luijkx, I. T. (2016). Warm spring reduced carbon cycle impact of the 2012 US summer drought. *Proceedings of the National Academy of Sciences of the United States of America*, 113, 5880–5885. <https://doi.org/10.1073/pnas.1519620113>
- Xia, J., Niu, S., Ciais, P., Janssens, I. A., Chen, J., Ammann, C., ... Luo, Y. (2015). Joint control of terrestrial gross primary productivity by plant phenology and physiology. *Proceedings of the National Academy of Sciences of the United States of America*, 112, 2788–2793. <https://doi.org/10.1073/pnas.1413090112>
- Xiao, J., Davis, K. J., Urban, N. M., & Keller, K. (2014). Uncertainty in model parameters and regional carbon fluxes: A model-data fusion approach. *Agricultural and Forest Meteorology*, 189, 175–186. <https://doi.org/10.1016/j.agrformet.2014.01.022>
- Zeng, N., Mariotti, A., & Wetzel, P. (2005). Terrestrial mechanisms of interannual CO<sub>2</sub> variability. *Global Biogeochemical Cycles*, 19, <https://doi.org/10.1029/2004GB002273>
- Zhou, S., Zhang, Y., Caylor, K. K., Luo, Y., Xiao, X., Ciais, P., ... Wang, G. (2016). Explaining inter-annual variability of gross primary productivity from plant phenology and physiology. *Agricultural and Forest Meteorology*, 226–227, 246–256. <https://doi.org/10.1016/j.agrformet.2016.06.010>
- Zhou, S., Zhang, Y., Ciais, P., Xiao, X., Luo, Y., Caylor, K. K., ... Wang, G. (2017). Dominant role of plant physiology in trend and variability of gross primary productivity in North America. *Scientific Reports*, 7, 41366. <https://doi.org/10.1038/srep41366>
- Zscheischler, J., Fatichi, S., Wolf, S., Blanken, P. D., Bohrer, G., Clark, K., ... Seneviratne, S. I. (2016). Short-term favorable weather conditions are an important control of interannual variability in carbon and water fluxes. *Journal of Geophysical Research: Biogeosciences*, 121, 2186–2198. <https://doi.org/10.1002/2016JG003503>

## SUPPORTING INFORMATION

Additional supporting information may be found online in the Supporting Information section at the end of the article.

**How to cite this article:** Fu Z, Stoy PC, Poulter B, et al.

Maximum carbon uptake rate dominates the interannual variability of global net ecosystem exchange. *Glob Change Biol*. 2019;25:3381–3394. <https://doi.org/10.1111/gcb.14731>